

Inhibition of Atrogin-1/MAFbx Expression by Adenovirus-Delivered Small Hairpin RNAs Attenuates Muscle Atrophy in Fasting Mice

Haolong Cong,^{1,2} Lunquan Sun,³ Changmei Liu,¹ and Po Tien¹

Abstract

Atrogin-1 or muscle atrophy F-box (MAFbx) is a major atrophy-related E3 ubiquitin ligase highly expressed in skeletal muscle during muscle atrophy and other disease states such as sepsis, cancer cachexia, and fasting. In this paper, we report experiments inhibiting MAFbx activity in fasting mice and in the skeletal myoblast cell line C2C12 via an adenovirus-mediated small hairpin RNA (shRNA) expression system in order to assess its suitability as a therapeutic target. Our results demonstrated that downregulation of MAFbx by shRNAs attenuated muscle loss induced by fasting in mice. Furthermore, we showed that when MAFbx expression was blocked both in cells and in fasting mice, the level of a myogenic factor, MyoD, was upregulated; whereas a muscle negative regulator, growth differentiation factor (GDF)-8 (myostatin), was suppressed. Our results also suggested that lower levels of MAFbx could also enhance muscle cell differentiation that corresponded to the reduced expression of GDF-8 and the increased level of MyoD. Taken together, the present study showed that MAFbx could be a potential molecular target for treating muscle atrophy.

Introduction

MUSCLE ATROPHY is characterized by a decrease in protein synthesis or an increase in protein degradation, which is a debilitating response found in many disease states and abnormal physiological conditions including cancer cachexia, starvation, diabetes, sepsis, denervation, muscle disuse, and muscular dystrophies (Stein and Wade, 2003). In this range of situations, muscle atrophy is thought to be due to increased expression of enzymes in the ubiquitin–proteasome proteolytic pathway. These include muscle-specific ubiquitin E3 ligase muscle atrophy F-box (atrogin-1/MAFbx) and muscle ring-finger protein-1 (MuRF1), important proteins in protein degradation (Cao *et al.*, 2005; Witt *et al.*, 2005). Studies have shown that these two proteins are induced dramatically during almost every kind of atrophy and play a critical role in mediating the loss of muscle protein (Gomes *et al.*, 2001; Attaix *et al.*, 2005). MAFbx is induced 8- to 40-fold in muscle atrophy during fasting, diabetes, cancer, and renal failure; up to 3-fold in hind limb suspension, immobilization, and denervation; and 10-fold in cachexia or dexamethasone administration models (Lecker *et al.*, 2004; Palma *et al.*, 2008). Mice lacking

MAFbx developed normal muscle but showed a significant attenuation of muscle atrophy (Bodine *et al.*, 2001). All these findings strongly suggested that MAFbx might be an ideal target for clinical intervention of muscle atrophy conditions.

A range of transcriptional and growth factors is also known to be involved in the regulation of muscle development. One of these, myostatin (growth differentiation factor [GDF]-8), is a major protein involved in regulating muscle growth and may be involved directly or indirectly in muscle-wasting conditions (Bogdanovich *et al.*, 2002). A secreted growth factor, GDF-8 acts as a negative regulator of skeletal muscle mass in mammals and other vertebrates, where it negatively regulates myocyte differentiation/growth and determines muscle size (Lee and McPherron, 2001; Dasarathy *et al.*, 2004). Mice lacking the GDF-8 gene have 25–30% greater muscle mass (McPherron *et al.*, 1997). Thus, blockade of GDF-8 could also hold great promise for the treatment of skeletal muscle atrophy. Indeed, our previous studies showed that downregulation of GDF-8 expression by synthetic antisense RNA oligonucleotides could lead to an increase in muscle mass in both normal and cancer cachectic mice (Liu *et al.*, 2008).

¹Center for Molecular Virology, CAS Key Laboratory of Pathogenic Microbiology and Immunology, Institute of Microbiology, Chinese Academy of Sciences, Beijing 100101, People's Republic of China.

²Graduate School of the Chinese Academy of Sciences, Beijing 100864, People's Republic of China.

³Faculty of Medicine, University of New South Wales, Sydney, NSW 2052, Australia.

In this paper, we examine MAFbx as a potential molecular target for treating muscle atrophy and provide some insight concerning the mechanism of regulation of muscle development and growth by MAFbx. For this, we established an adenovirus-based MAFbx-specific small hairpin RNA (shRNA) delivery system that could efficiently express and deliver shRNAs in fasting mice. Our results demonstrated that this adenovirally delivered shRNA could decrease the expression of MAFbx in fasting mice and C2C12 cells. At the same time, we observed that inhibition of MAFbx could induce cell differentiation in both fasting mouse muscle and C2C12 cells, leading to an increase in muscle mass and type II muscle fiber size in fasting mice. In addition, our studies showed that MAFbx suppression attenuated the down-regulation of MyoD, a myogenic factor, and decreased the expression of GDF-8. This study forms the basis for further understanding of the mechanisms of muscle atrophy in various diseases and for developing nucleic acid-based therapeutics for muscle-wasting conditions.

Materials and Methods

Cell culture and animals

Mouse skeletal muscle cell line C2C12 and the packaging cell line M293 were propagated and maintained in Dulbecco's modified Eagle's medium (DMEM) supplemented with antibiotics, and 10% fetal bovine serum at 37°C in the presence of 5% CO₂. To induce differentiation, confluent C2C12 cells were propagated in DMEM supplemented with antibiotics and 2% horse serum for the indicated period. Cells were transfected with FuGENE HD transfection reagent (Roche, Indianapolis, IN) according to the manufacturer's instructions. A control plasmid, pDC316-EGFP, was used to determine the transfection efficiency.

Four-week-old female BALB/c mice were purchased from the Laboratory Animal Center of the Chinese Academy of Military Medical Sciences (Beijing, People's Republic of China). They were housed at a constant temperature under a 12 hr:12 hr light-dark cycle and given free access to water and food for 1 week before experiments were performed. All animal experiments were undertaken within the guidelines of the Chinese Academy of Sciences regulations for the use of experimental animals.

Construction of the vectors

The human RNA polymerase (Pol) III H1 promoter and U6+27 promoter, the latter containing 27 additional nucleotides upstream of the specific hairpin, were used in this study. A cassette containing the human U6+27 promoter and H1 promoter derived from the Super hU6+27+H1 plasmid by digestion with *KpnI* and *EcoRI* was cloned into the same restriction sites of the pUC18 plasmid, and the hU6+27+H1 cassette in pUC18-hU6+27+H1 was ligated to the *XbaI* and *EcoRI* sites of pDC312 (VGTC, Beijing, China) to obtain the plasmid pDC312-hU6+27+H1.

Three shRNAs targeting a homologous 3' region of mouse MAFbx genes and a control shRNA (designated shHBC) targeting the hepatitis B virus core antigen gene were designed. To facilitate the formation and processing of shRNAs, a loop sequence (CTCTTGA) was designed in the middle area of all shRNAs. The sequences of the three 61-nucleotide-long

mouse-specific shRNAs were as follows: shMAFbx-1 (nucleotide positions 538–559, AW051824), 5'-GAT CAA AAA CGA AGG AGC GCC ATG GAT ATT CAA GAG ATA TCC ATG GCG CTC CTT CGT TTT T-3'; shMAFbx-2 (nucleotide positions 802–823), 5'-GAT CAA AAA CCA ACA ACC CAG AGA GCT GTT CAA GAG ACA GCT CTC TGG GTT GTT GGT TTT T-3'; and shMAFbx-3 (nucleotide positions 1126–1147), 5'-GAT CAA AAA GAC AAA GGG CAG CTG GAT TTT CAA GAG AAA TCC AGC TGC CCT TTG TCT TTT T-3'. These sequences are homologous to the corresponding sequences of the human MAFbx mRNA. The complementary oligonucleotides were also synthesized to produce DNA duplexes corresponding to each of the shRNAs. All shRNA oligonucleotides were annealed and ligated to the *BglIII* and *SalI* sites located between the hU6+27 promoter and the H1 promoter to produce recombinant vectors pDC312-hU6+27+siMAFbx-1+H1, pDC312-hU6+27+siMAFbx-2+H1, pDC312-hU6+27+siMAFbx-3+H1, pDC312-hU6+27+H1, and pDC312-hU6+27+siHBC+H1, which were confirmed by DNA sequencing.

Generation of recombinant adenovirus

The AdMax system (VGTC) was used to generate recombinant adenoviral vectors. M293 cells were plated at 4×10^5 per well in six-well plates. On the next day, the cells were cotransfected with 2 μ g of each recombinant vector and 0.2 μ g of adenoviral genomic plasmid, by using 8 μ l of FuGENE HD transfection reagent to generate the recombinant adenovirus. Seven days after transfection, the cells and culture fluid containing the recombinant adenovirus were collected, frozen, and thawed at –80°C and 37°C, respectively, three times. The cell lysates were centrifuged at 3000 \times g for 5 min and the supernatants containing recombinant adenovirus were stored at –80°C. To verify the constructs, the viral DNA was purified and amplified by polymerase chain reaction (PCR) over 35 cycles of denaturation at 94°C for 30 sec, primer annealing at 55°C for 30 sec, and extension at 72°C for 1 min, using primers 5'-TCT AGG TGT TTT CCG CGT TCC (sense) and 5'-TCT TCG AGT CGA GGA TCC G (antisense). PCR products were identified by electrophoresis on a 1.0% agarose gel and the fragments were gel purified and sequenced by AuGCT (Beijing, China).

Virus propagation and titer determination

M293 cells (1×10^7) were plated in each 15-cm plate. Six plates were used to propagate each recombinant adenovirus according to the manuals provided with the AV precipitation purification kit (GenMed, Beijing, China). On the next day, 1 ml of each recombinant adenovirus was added to each plate of M293 cells. The growth medium was replaced with fresh medium after 24 hr of incubation. Three days later, the adenovirus was purified, condensed to 1 ml, and stored at –80°C. Viral titers were determined in triplicate by means of a rapid adenovirus titer detection kit (VGTC), according to the instruction manual.

Transduction of C2C12 cells with recombinant adenovirus

C2C12 cells were plated at 2×10^5 cells per well in six-well plates. On the next day, when the cells were approximately

50% confluent, recombinant virus was added to each well. After 12 hr of transduction, the growth medium was replaced with differentiation medium as described previously. After 24 hr of differentiation, the transduced cells were subjected to further analysis by PCR, Western blotting, cell staining, and Northern blotting as described subsequently.

Cell staining and fluorescence assays

Transduction of C2C12 cells with recombinant adenovirus was performed as described previously. Cells were then washed gently with phosphate-buffered saline (PBS) twice and fixed in 4% paraformaldehyde for 10 min at 37°C, followed by three washes with PBS. For cell membrane staining, 1 μ l of 1,1'-dioctadecyl-3,3,3',3'-tetramethylindocarbocyanine perchlorate (DiI C18; Biotium, Hayward, CA) stock solution (2 mg/ml) was added to each well, making a final concentration about 2 μ mol/liter. Cells were stained for 15 min at 37°C, followed by three washes with PBS. Cell nuclei were stained with 2-(4-amidinophenyl)-6-indolecarbamidine dihydrochloride (DAPI; Sigma-Aldrich, St. Louis, MO) and examined with a Nikon inverted fluorescence microscope, using excitation wavelengths of 549 and 355 nm.

Development of a suitable fasting model for injection of mice with recombinant adenoviral vectors

Four-week-old female BALB/c mice weighing 10 to 13 g were divided into eight groups ($n=3$). At commencement, they were deprived of solid food but given free access to water for 12, 24, 36, 48, 60, and 72 hr, respectively. The mice were then given 2 g of sterilized feedstuff per mouse each day to keep them at a nutritionally restricted level. After 7 days of fasting, the leg muscles including the quadriceps (rectus femoris), gastrocnemius, triceps, and extensor digitorum longus (EDL) were dissected and weighed. Gastrocnemius muscle were collected and used for protein extraction and analysis.

Injection of mice with recombinant adenoviral vectors

Mice were divided into four groups, namely A, B, C, and D ($n=6$). Group D, unfasted and injected mice, was fed under normal conditions throughout the experimental period. At commencement, each mouse in group A (siMAFbx), group B (empty vector), and group C (mock) was injected on days 1 and 3, with each injection (250 μ l) containing 1×10^{10} IU of siMAFbx recombinant adenovirus, 1×10^{10} IU of pDC312 recombinant adenovirus, and saline, respectively. After the first injection, each mouse in groups A, B, and C was given free access to water and 2 g of sterilized feedstuff each day and kept at a nutritionally restricted level. The mice were weighed every day during the treatment period. Seven days after the last injection, the thigh muscles including the quadriceps (rectus femoris), gastrocnemius, triceps, and EDL were dissected and weighed. Gastrocnemius were used fresh for protein and mRNA extraction and analysis.

Real-time PCR

Total RNA was extracted from cells or tissues with TRIzol (Invitrogen, Carlsbad, CA). RNA was separated electrophoretically on agarose gels under denaturing conditions in

order to confirm the integrity of ribosomal RNA bands. RNA concentration was quantified with a GeneQuant spectrophotometer (GE Healthcare Life Sciences, Piscataway, NJ) at 260 nm. Single-stranded cDNA synthesis was carried out from 2 μ g of total RNA by reverse transcription (RT) (Promega, Madison, WI). Real-time fluorescence quantitative PCR was performed in an Applied Biosystems Prism 7000 instrument in reactions containing an Applied Biosystems SYBR green master mix reagent (Applied Biosystems, Foster City, CA) and oligonucleotide primer pairs corresponding to the endogenous control β -actin gene and MAFbx, GDF-8, and MyoD cDNAs. The reagents were denatured at 95°C for 10 min, followed by 40 cycles of 15 sec at 95°C and 60 sec at 60°C. The sequences of the primers were as follows: β -actin—forward, 5'-GAA CCC TAA GGC CAA CCG TGA A-3'; reverse, 5'-CTC AGT AAC AGT CCG CCT AGA A-3'; MyoD—forward, 5'-GCA AGA CCA CCA ACG CTG AT-3'; reverse, 5'-GGT TCG GGT TGC TGG ACG TG-3'; GDF-8—forward, 5'-CAG ACC CGT CAA GAC TCC TAC A-3'; reverse, 5'-CAG TGC CTG GGC TCA TGT CAA G-3'; MAFbx—forward, 5'-GCA GAG AGT CGG CAA GTC-3'; reverse, 5'-CAG GTC GGT GAT CGT GAG-3'. The results were expressed as expression of the gene of interest relative to the expression of the β -actin internal control gene (C_t of gene of interest minus C_t of internal control gene). Calculation of relative changes in the expression level of one specific gene ($\Delta\Delta C_t$) was performed by subtraction of mean ΔC_t of the control group from ΔC_t of each sample of the experimental groups. Last, the relative expression value, normalized to an endogenous reference, was given by: $2^{-\Delta\Delta C_t}$ with $\Delta\Delta C_t \pm$ SEM, where SEM is the standard error of the mean of the $\Delta\Delta C_t$ value (*User Bulletin 2*; Applied Biosystems).

Western blotting

Total proteins of C2C12 cells were extracted with lysis buffer containing 100 mM Tris-HCl, 0.05% IGEPAL CA-630, phenylmethylsulfonyl fluoride (100 μ g/ml), dithiothreitol (DTT, 100 μ g/ml), aprotinin (1 μ g/ml), and leupeptin (1 μ g/ml). Gastrocnemius muscles were homogenized in radioimmunoprecipitation assay (RIPA) buffer (BioMed, Beijing, China), incubated for 30 min on ice, and centrifuged at $15,000 \times g$ for 10 min at 4°C, and the supernatants were collected. The protein concentration of each sample was measured by the Bradford method (Bio-Rad, Hercules, CA). Equal amounts of protein (50 μ g) were heat-denatured in sample-loading buffer (50 mM Tris-HCl [pH 6.8], 100 mM DTT, 2% sodium dodecyl sulfate [SDS], 0.1% bromophenol blue, and 10% glycerol), separated by SDS-polyacrylamide gel electrophoresis (10% polyacrylamide, 0.1% SDS), and electroblotted to a polyvinylidene difluoride membrane. The membrane was blocked with 5% skim milk in TBST buffer (50 mM Tris-HCl, 100 mM NaCl, and 0.1% Tween 20, pH 7.4) and incubated for 90 min at 37°C with the following selected antibodies: polyclonal anti-MAFbx diluted at 1:1000 (ECM Biosciences, Versailles, KY), monoclonal anti-MyoD diluted at 1:2000 (BD Biosciences, San Jose, CA), anti-GDF-8 diluted at 1:500 (Santa Cruz Biotechnology, Santa Cruz, CA), monoclonal anti-myogenin diluted at 1:200 (BD Biosciences), monoclonal anti- α -actin diluted at 1:100 (Santa Cruz Biotechnology), monoclonal anti-myosin diluted at 1:100 (Santa Cruz Biotechnology), anti- β -actin diluted at 1:2500 (Santa

Cruz Biotechnology), anti-c-Fos diluted at 1:1000 (Santa Cruz Biotechnology), anti-NF- κ B diluted at 1:1000 (Santa Cruz Biotechnology), and polyclonal to adenovirus type 5 diluted at 1:2000 (Abcam, Cambridge, UK). The signals were visualized by subsequent chemiluminescence reaction with the corresponding horseradish peroxidase-conjugated IgG (1:3000) in the ECL system (Appligen Technologies, Beijing, China). The image and data were analyzed with Quantity One version 4.6.2 software (Bio-Rad). The expression of β -actin and β -tubulin was used for loading normalization.

Northern blotting

C2C12 cells were washed three times with ice-cold PBS and mouse gastrocnemius muscle, cardiac muscle, liver, lungs, spleen, and kidney were ground to powder in liquid nitrogen for Northern blot analysis. The samples were extracted in TRIzol (Invitrogen); the total RNA obtained was dissolved in 50% deionized formamide (Amresco, Solon, OH) and separated electrophoretically on 1% agarose gels under denaturing conditions to confirm the integrity of ribosomal RNA bands. The RNA concentration of each sample was measured with a GeneQuant spectrophotometer at 260 nm. Total RNA (100 μ g) was separated on polyacrylamide gels (17.5% polyacrylamide, 8 M urea, 0.09 M Tris, 0.09 M boric acid, 2 mM Na₂EDTA, pH 8.3). Separated RNA in gel was electroblotted onto Hybond-N+ membrane (GE Healthcare) with a Trans-Blot SD semi-dry electrophoretic transfer cell (Bio-Rad). Oligonucleotides with the same se-

quence as siMAFbx-1 were synthesized to use as probes for the small interfering RNA (siRNA) (5'-TAT CCA TGG CGC TCC TTC GT-3') and U6 promoter (5'-GCA GGG GCC ATG CTA ATC TTC TCT GTA TCG-3'). After ultraviolet cross-linking, the blotted membrane was prehybridized with hybridization buffer at 37°C for 60 min, and then hybridized at 37°C overnight with α -³²P-labeled antisense probes prepared using T₄ polynucleic kinase (Takara Bio, Dalian, China). The membrane was washed twice for 20 min at 37°C with 2 \times saline-sodium citrate (SSC) containing 1% SDS and twice for 15 min with 1 \times SSC and 1% SDS and exposed to X-ray film (Kodak, Rochester, NY) at -80°C for signal visualization.

Histological analysis of muscle fibers

Gastrocnemius muscles were removed from the mice, fixed in formalin, and embedded in paraffin. Paraffin sections (2-4 μ m) were stained with hematoxylin and eosin for fiber counting and cross-sectional area measurement. ATPase staining was performed to differentiate the muscle fiber types (Green *et al.*, 1982). Quantitative evaluation of stained sections for myofiber size was performed with Image-Pro 6.0 program software (Media Cybernetics, Silver Spring, MD), coupled to a Nikon 80I microscope equipped with a Nikon DS-L1 digital camera, calibrated for spatial measurement and intensity. Fiber size was determined by measuring the area of each transverse myofiber per unit area.

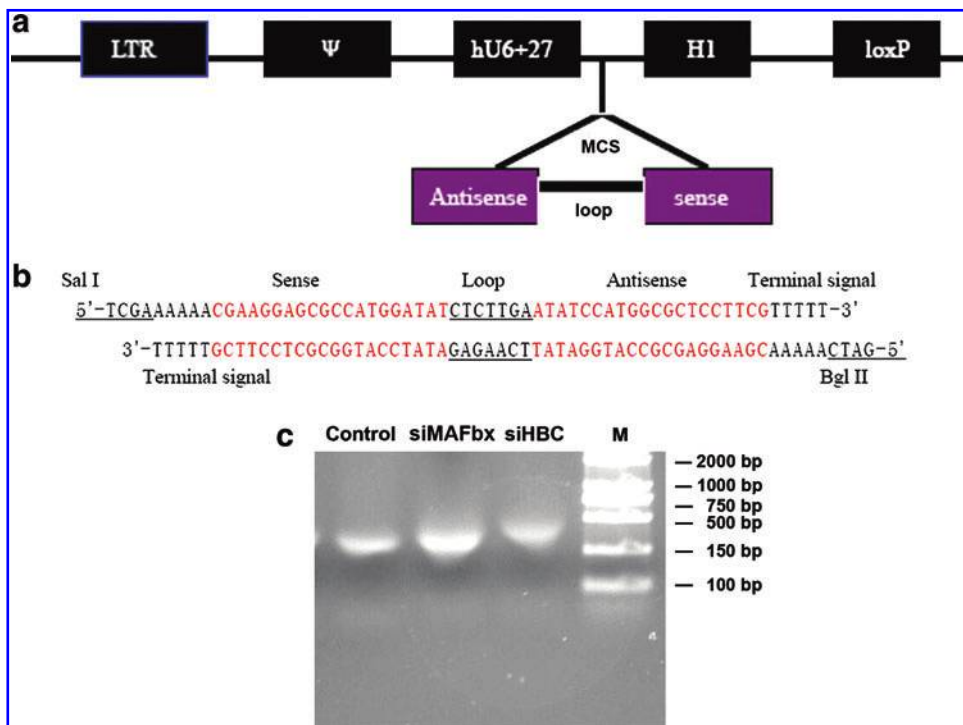


FIG. 1. Construction of an adenoviral vector-mediated shRNA delivery system. A cassette containing the human U6+27 promoter and H1 promoter was inserted into the multiple cloning site of the pDC312 plasmid to generate the recombinant expression vector pDC312-hU6+27+H1. DNA duplexes corresponding to the designed shRNAs were ligated to the *Bgl*II and *Sal*I sites between the hU6+27 promoter and H1 promoter of this vector. The final adenoviral vectors were generated when the recombinant expression vectors were cotransfected with adenoviral genomic plasmid into M293 cells. (a) Schematic representation of the recombinant expression vector pDC312-hU6+27+H1. Ψ , extended packaging signal; LTR, long-terminal repeat; MCS, multiple cloning sites;

H1, polymerase III H1 promoter; hU6+27, polymerase III U6 promoter containing 27 additional nucleotides upstream of the specific hairpin. (b) The sequence of siMAFbx oligonucleotides inserted into the adenoviral vectors. (c) PCR analysis of inserts from the adenoviral vectors. siMAFbx and siHBC represent the adenoviruses that were generated from pDC312-hU6+27+siMAFbx-1+H1 and pDC312-hU6+27+siHBC+H1 expression vectors, respectively. Control is the virus that was integrated with the pDC312-hU6+27+H1 empty vector only; M, marker lane (DL-2000; ShineGene Molecular Biotech, Shanghai, China). Color images available online at www.liebertonline.com/hum.

Statistical analysis

Data were subjected to one-way analysis of variance with factors of treatment and expressed as means plus SD. Comparisons between two groups were performed by an unpaired Student *t* test. Values were considered significantly different when $p < 0.05$.

Results

Optimization of the adenoviral vector system for shRNA delivery

In this study, a recombinant pDC312 *lox* shuttle plasmid for Cre-based Ad vector rescue was constructed to drive high levels of transient expression of the small hairpin RNA (shRNA) under the direction of both the RNA Pol III promoter of human U6+27 and the H1 small nuclear RNA promoter inserted in reverse orientation to each other (Fig. 1a). The configuration of the constructs and the sequences of the inserted oligonucleotides siMAFbx-1, siMAFbx-2, and siMAFbx-3 (Fig. 1b) targeting the mouse MAFbx mRNA were confirmed by DNA sequencing.

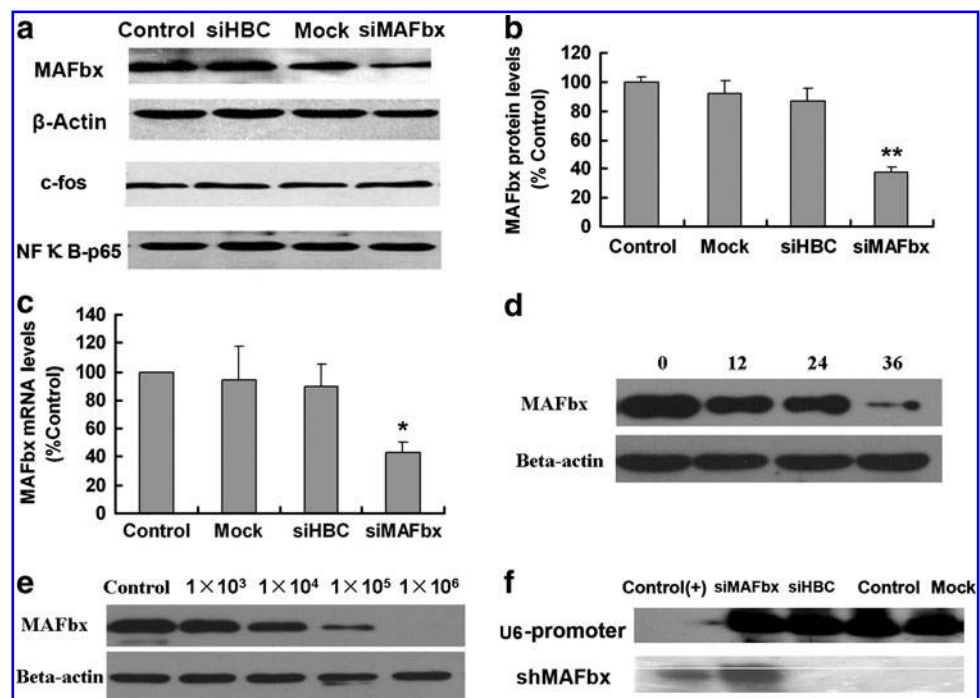
The siRNA construct that is most effective in inhibiting MAFbx expression was identified by Western blot analysis of MAFbx protein expression in C2C12 cells before and after vector transfection. Results showed that before transfection, the MAFbx expression level was upregulated gradually after differentiation (data not shown). After transfection, only siMAFbx-1 could significantly downregulate the expression of the target gene (data not shown). Therefore, vector pDC312-hU6+27+siMAFbx-1+H1 was used to generate the recom-

binant adenoviral vector. Sequencing of the siMAFbx-1 PCR fragment obtained from the recombinant adenovirus (Fig. 1c) demonstrated that the shRNA fragment was integrated into the vector with the correct orientation and sequence.

Gene-silencing effect of siMAFbx in C2C12 cells

To examine whether siMAFbx-1 recombinant adenovirus infection could lead to the downregulation of MAFbx gene expression in the C2C12 cell line, Western blotting and real-time PCR were performed to measure the MAFbx expression level in infected C2C12 cells. Results showed that the MAFbx protein level was significantly reduced in siMAFbx recombinant adenovirus-infected cells (62.76%) compared with control (Fig. 2a and b), whereas no inhibiting effect was observed in cells infected with the siHBC adenoviral vector. RT-PCR results showed that the reduction of MAFbx mRNA was 57.37% in C2C12 cells infected with siMAFbx adenoviruses (Fig. 2c), compared with the control. The time course of MAFbx expression mediated by siMAFbx-1 in C2C12 cells was also analyzed; results show that with the prolonged time of siMAFbx-1 recombinant adenovirus infection, MAFbx expression in C2C12 cells decreased gradually (Fig. 2d). Further evidence shows that the downregulation of MAFbx expression in C2C12 cells was dependent on the siMAFbx-1 recombinant adenovirus dose (Fig. 2e). Northern blots further demonstrated that the designed siRNA was highly expressed in the infected C2C12 cells (Fig. 2f). These data confirmed that the adenovirus-delivered shRNAs were efficiently expressed and inhibited the expression of MAFbx in C2C12 cells. To examine whether there was any nontarget effect of the

FIG. 2. Inhibition of MAFbx in C2C12 cells by adenovirus-delivered siMAFbx. C2C12 cells transduced with recombinant adenovirus were analyzed by Western blot, real-time PCR, and Northern blot as described in Materials and Methods to measure the MAFbx expression level in recombinant adenovirus-infected C2C12 cells. Control, uninfected C2C12 cells; Mock, cells infected with pDC312-hU6+27+H1 recombinant adenovirus; siHBC, cells infected with siHBC recombinant adenovirus. (a) Western blot of C2C12 cells. (b) Quantitation of MAFbx expression in C2C12 cells. **Significant difference at $p < 0.02$ compared with control. (c) Quantitative RT-PCR analysis of MAFbx in C2C12 cells. *Significant difference at $p < 0.05$ compared with control. (d) Time course of MAFbx expression mediated by siMAFbx-1 in the C2C12 cell line; 0, 12, 24, and 36 (hours) represent the time after siMAFbx-1 transduction. (e) MAFbx expression in C2C12 cells with various siMAFbx-1 recombinant adenovirus doses. 1×10^3 , 1×10^4 , 1×10^5 , and 1×10^6 (IU) represent the quantity of siMAFbx-1 recombinant adenovirus used in cell transduction. (f) Northern blot analysis of C2C12 cells; Control(+), lane loaded with an antisense oligonucleotide of designed siMAFbx. Data are presented as means + SD, based on three independent experiments.



expressed shRNA, we also analyzed the expression of two important transcriptional factors, NF- κ Bp65 and c-Fos, in C2C12 cells. The results showed that the expression of anti-MAFbx shRNA did not impact on these genes (Fig. 2a).

Inhibition of MAFbx expression by adenovirus-delivered shRNAs in fasting mice

A suitable mouse fasting model to mimic the pathological phenotypes of muscle atrophy was established for studying the biological effect of shRNA delivered by adenoviral vectors. To validate the model, we first analyzed the expression profile of MAFbx protein in fasting mice. The results showed that MAFbx expression was upregulated gradually after fasting commenced (Fig. 3a and b). MAFbx protein levels in muscles at 12 hr was about 45% higher compared with the unfasted control group, and peaked, at 60 hr, at a level that was three times higher than in the unfasted mice. In fasting mice, the body and muscle weights, and the ratio of muscle mass to body weight, were all shown to decrease gradually

(Fig. 3c–e). Notably, this reduction in body and muscle weights was consistent with the change in MAFbx expression in muscle, indicating that the model showed some characteristic features of muscle atrophy.

To investigate whether adenovirus-delivered siMAFbx could downregulate MAFbx expression *in vivo* and impact on muscle growth, we injected siMAFbx recombinant adenovirus into fasting mice via the tail vein. Seven days after the second injection, gastrocnemius muscles were collected and analyzed for MAFbx protein levels. Our results showed that the MAFbx protein level in the siMAFbx recombinant adenovirus-treated group decreased by 66.8% compared with the control group (Fig. 4a and b), whereas no reduction was observed in the mock group. To investigate whether siMAFbx small hairpin RNAs were transcribed in the injected mice, total RNAs from gastrocnemius muscle were extracted and Northern blotting analysis was performed. As expected, transcripts of small hairpin RNAs of siMAFbx in mouse muscle were detected in the siMAFbx-treated group, but not in the saline and pDC312 empty

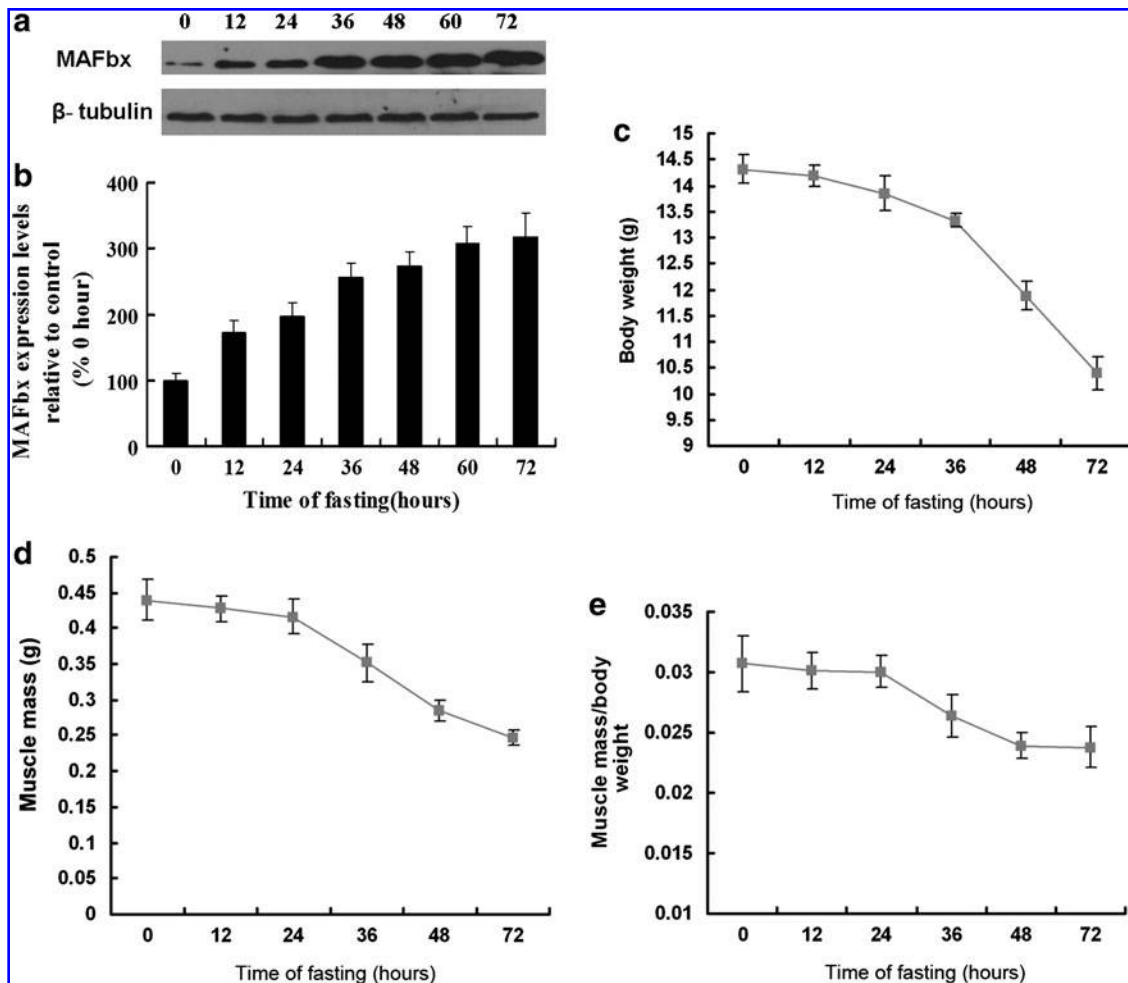


FIG. 3. Establishment of a suitable mouse fasting model for adenovirus-mediated delivery of siMAFbx. BALB/c mice were fasted for various periods of time and then placed on a restricted diet as described in Materials and Methods. (a) Western blot analysis of MAFbx expression in the gastrocnemius muscle of unfasted mice and mice fasted for injection. (b) Quantitation of the MAFbx expression level in mouse gastrocnemius muscle as measured with Quantity One software (Bio-Rad). Mice were fasted for various periods of time as indicated. (c) Changes in mouse body weight in fasted mice. (d) Changes in mouse muscle mass in fasted mice. (e) The ratio of mouse muscle mass to body weight in fasted mice. Data are presented as means \pm SD ($n = 3$ per experiment).

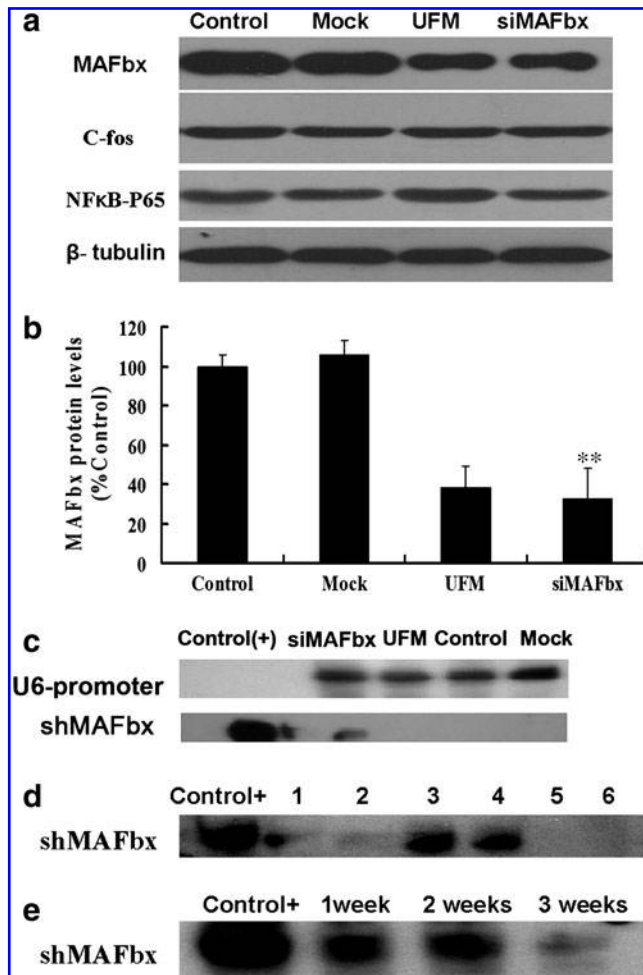


FIG. 4. Inhibition of MAFbx expression by adenovirus-delivered shRNAs in a fasting mouse model. Recombinant adenoviruses were transduced into mice on days 1 and 3 as described in Materials and Methods. Control, fasting mice injected with saline; Mock, fasting mice transduced with pDC312 recombinant adenovirus (empty vector); UFM, unfasted and uninjected mice; siMAFbx, fasting mice transduced with siMAFbx recombinant adenovirus. (a) Western blot analysis of the effect of siMAFbx on the expression level of MAFbx in mouse gastrocnemius muscle. (b) Quantitation of the effect of siMAFbx on the expression level of MAFbx in mouse gastrocnemius muscle. **Significant difference at $p < 0.02$ compared with control. (c) Northern blot analysis of the expression of siMAFbx in gastrocnemius muscle of fasting mice; Control(+), lane loaded with an antisense oligonucleotide corresponding to the designed siMAFbx. Data are presented as means and SD based on three independent experiments ($n = 6$ per experiment). (d) Northern blot analysis of the expression of siMAFbx in various mouse tissues. Lane 1, gastrocnemius muscle; lane 2, liver; lane 3, cardiac muscle; lane 4, spleen; lane 5, kidney; lane 6, lungs. (e) The time course of MAFbx expression in mice after siMAFbx-1 recombinant adenovirus transduction.

vector control groups (Fig. 4c). The distribution of hairpin RNAs of siMAFbx in mouse gastrocnemius muscle, cardiac muscle, liver, lungs, spleen, and kidney was further analyzed by Northern blotting; results showed that the transcription of siMAFbx was detected mainly in gastrocnemius

muscle, cardiac muscle, liver, and spleen (Fig. 4d). Further evidence showed that the transcription of siMAFbx in mouse muscle could last at least 3 weeks after the last injection (Fig. 4e). Taken together, these results indicate that the designed siMAFbx was expressed in mouse muscle and efficiently inhibited the expression of MAFbx in fasted mice.

Adenovirus-delivered shRNAs targeted to MAFbx attenuate muscle atrophy in fasting mice

To evaluate whether the downregulation of MAFbx could attenuate the loss of muscle mass in fasting atrophy, fasting mice were injected with the recombinant adenoviruses and saline as described previously and muscle tissues were collected and weighed 7 days after the last injection. Results showed that the muscle weight in the group treated with the siMAFbx recombinant adenovirus was increased by 28.87% relative to the saline and empty vector control groups (Fig. 5a). When the ratio of muscle mass to body weight was measured, a similar increase was observed with siMAFbx treatment (Fig. 5b). This suggested that the siMAFbx recombinant adenovirus targeted to MAFbx inhibited MAFbx expression *in vivo* and increased muscle mass in fasted mice in our muscle atrophy model.

To investigate whether the increase in muscle weight is the result of an increase in muscle fiber size, we also examined the cross-sectional area of the gastrocnemius muscle in the experimental mice. Hematoxylin and eosin stain results showed that the mean cross-sectional area of fibers of siMAFbx recombinant adenovirus-treated fasted mice was 27.45% larger than that of fibers of saline- and empty vector-treated fasted mice (Fig. 5c and d). ATPase staining demonstrated that the cross-sectional area of type II muscle fibers of the siMAFbx vector-treated group increased by about 16.5% compared with the saline and empty vector control groups (Fig. 5e and f), whereas no significant change in type I muscle fibers was observed. These data provide strong evidence that downregulation of MAFbx could attenuate muscle mass loss in fasting mice and that this effect occurs predominantly in type II muscle fibers.

Inhibition of MAFbx expression reactivates myogenic differentiation in fasting mice

MAFbx works coordinately with proteasomes and degrades a series of proteins during muscle atrophy (Palma *et al.*, 2008). Low expression levels of MAFbx may limit protein breakdown in muscle wasting and lead to the regeneration of muscle fibers. To determine whether the level of MAFbx expression affects the ability of myogenic cells to differentiate, we first examined the effect of siMAFbx on the differentiation of C2C12 cells. After transduction with siMAFbx, pDC312, and siHBC recombinant adenoviruses, C2C12 cells were induced to differentiate for 24 hr and then examined by Western blotting for the specific differentiation markers myogenin, α -actin, and myosin. As shown in Fig. 6, the ability of siHBC and pDC312 adenovirus-infected C2C12 cells to differentiate terminally is almost nonexistent, as shown by the weak expression of specific differentiation markers (Fig. 6a). By contrast, the siMAFbx adenovirus-infected cells exhibited an induction of differentiation, as demonstrated by a 13-fold increase in

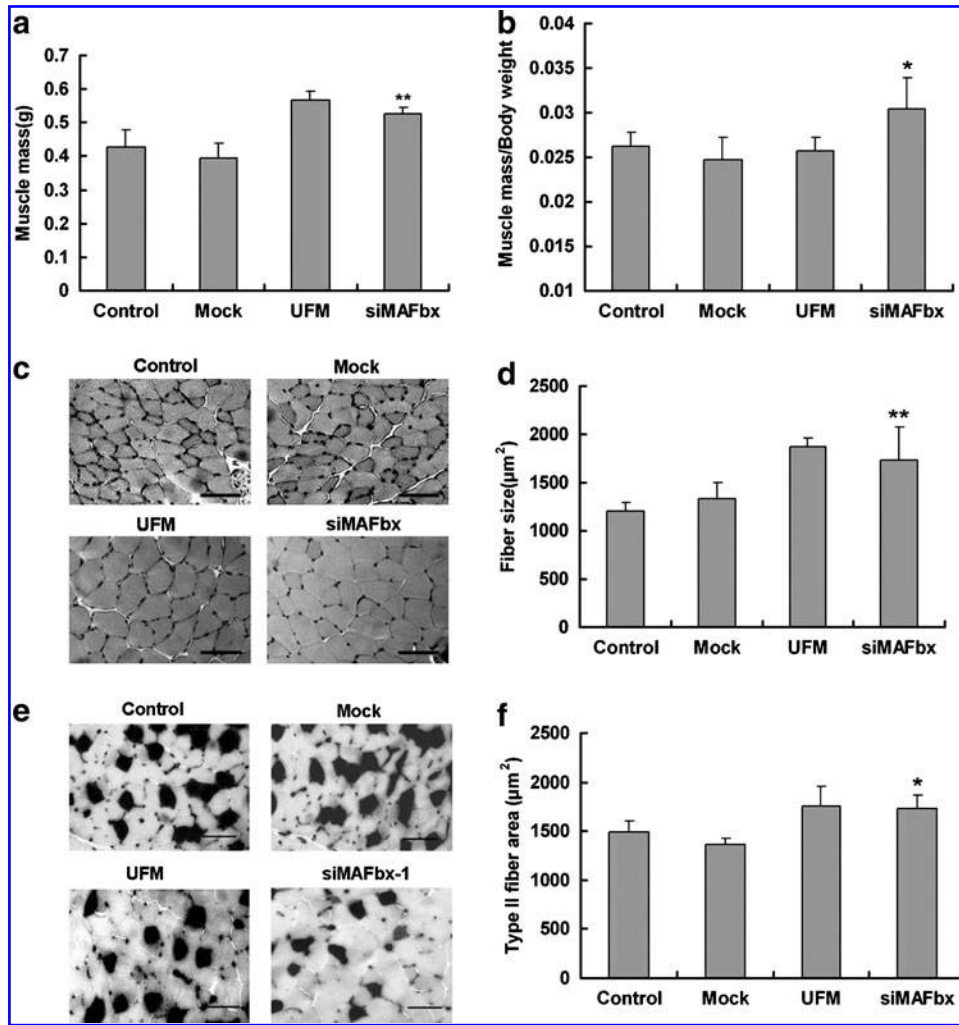


FIG. 5. Effects of adenovirus-delivered siRNA on muscle mass and muscle fiber size in fasting mice. The gastrocnemius muscle of transduced mice was fixed and stained for fiber analysis as described in Materials and Methods. Control, fasting mice injected with saline; Mock, fasting mice transduced with pDC312 recombinant adenovirus (empty vector); UFM, unfasted and uninjected mice. (a) Changes in mouse muscle mass. **Significant difference at $p < 0.02$ compared with control. (b) The ratio of muscle mass to body weight. *Significant difference at $p < 0.05$ compared with control. (c) Representative micrograph of gastrocnemius muscle fibers. Scale bars: $100 \mu\text{m}$. (d) Quantitation of gastrocnemius muscle fiber cross-sectional area determined by image analysis of six fields for each tissue section, totaling 600–800 fibers per treatment. **Significant difference at $p < 0.02$ compared with control. (e) Myofibrillar ATPase-stained muscle cross-sections. Fiber types were determined by staining intensity; type I > type II (from dark to light). Scale bars: $100 \mu\text{m}$. (f) Quantitation of type II fiber areas in gastrocnemius cross-sections. *Significant difference at $p < 0.05$ compared with control. Data are presented as means and SD ($n = 6$).

myogenin content (Fig. 6b), a 15-fold increase in α -actin (Fig. 6c), and a 28-fold increase in myosin (Fig. 6d). Some multinucleated myotube-like structures were also shown to be developing in the siMAFbx-infected cells after 24 hr of culture (Fig. 6e). These results indicated that downregulation of the MAFbx protein could override the differentiation block in C2C12 cells.

We next examined changes in the differentiation markers in fasting mice injected with the various adenoviral vectors. A Western blot (Fig. 6f) of gastrocnemius muscle showed that there was an induction of differentiation in the siMAFbx treatment group, as the expression levels of α -actin and myogenin were increased by 42.73% (Fig. 6g) and 50.69% (Fig. 6h), respectively, compared with controls. These results

demonstrated that a reduced level of MAFbx could induce differentiation of muscle fibers in fasted mice.

Effects of adenovirus-delivered shRNA targeted to MAFbx on MyoD and GDF-8 expression in fasting mice

GDF-8 and MyoD are two of the most important regulators in myoblast differentiation and muscle growth (Liu *et al.*, 2008). Because studies have shown that MAFbx can interact with and degrade MyoD (Tintignac *et al.*, 2005), we suspect that downregulation of MAFbx may affect negative regulators such as GDF-8 and positive regulators such as MyoD. To test this hypothesis, we examined the expression levels of GDF-8 and MyoD in gastrocnemius muscle of

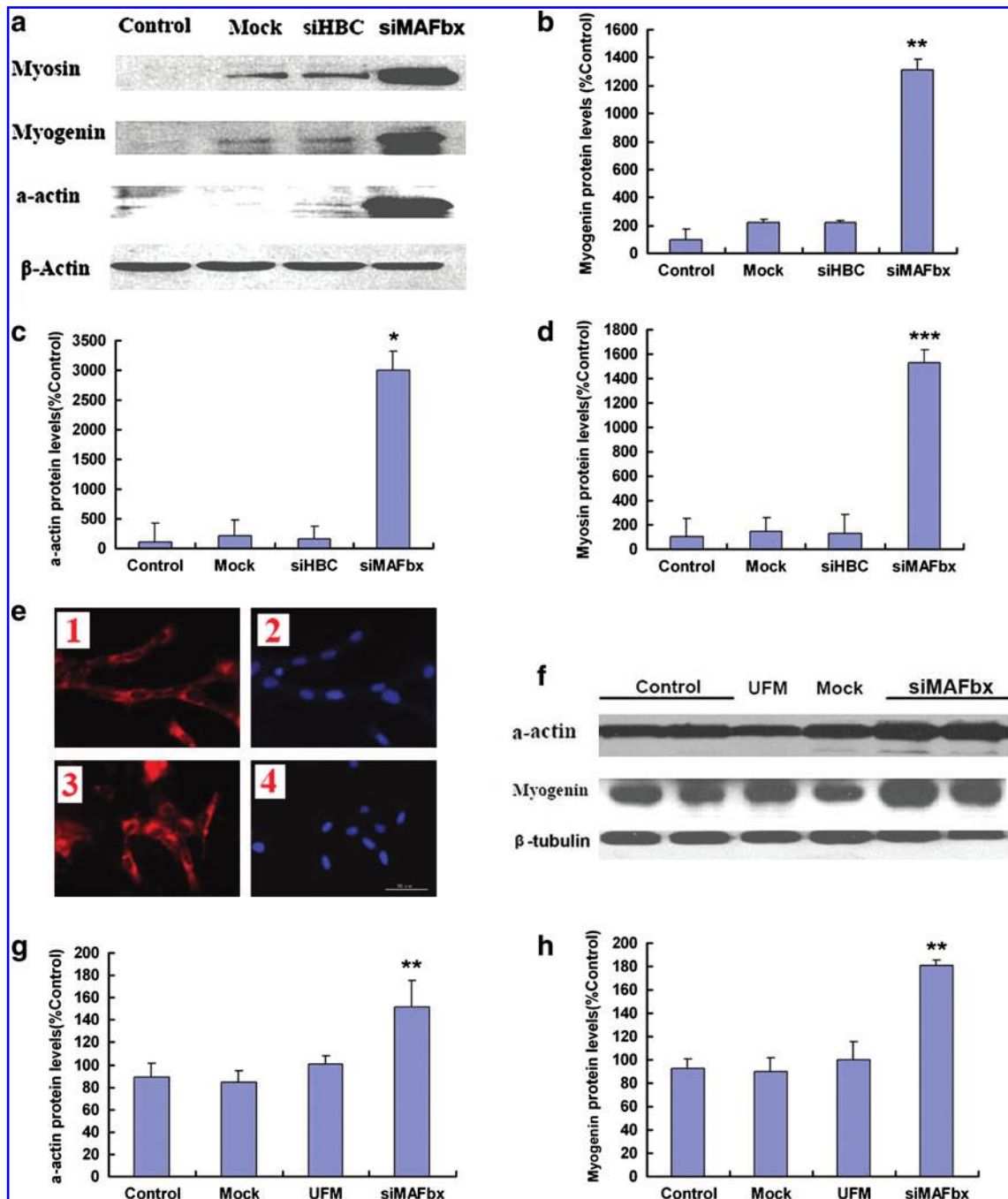


FIG. 6. Effects of the inhibition of MAFbx expression on myogenic differentiation of C2C12 cells and fasting mice. (a) Western blot analysis of myosin, α -actin, and myogenin in C2C12 cells. Control, uninfected C2C12 cells; Mock, cells infected with pDC312 recombinant adenovirus (empty vector); siHBC, cells infected with siHBC recombinant adenovirus. (b) Quantitation of myogenin expression level in C2C12 cells. **Significant difference at $p < 0.02$ compared with control. (c) Quantitation of α -actin expression level in C2C12 cells. *Significant difference at $p < 0.05$ compared with control. (d) Quantitation of myosin expression level in C2C12 cells. ***Significant difference at $p < 0.001$ compared with control. (e) DiI and DAPI staining of C2C12 cells. Panels 1 and 2 represent the DiI and DAPI staining of C2C12 cells after siMAFbx-1 recombinant adenovirus transduction, respectively; panels 3 and 4 represent the DiI and DAPI staining of C2C12 cells after siHBC recombinant adenovirus transduction, respectively. (f) Western blotting analysis of myogenin and α -actin in gastrocnemius muscle of fasting mice. Control, fasting mice injected with saline; Mock, fasting mice transduced with pDC312 recombinant adenovirus (empty vector); UFM, unfasted, uninjected mice. (g) Quantitation of the α -actin expression level in gastrocnemius muscle of fasting mice. **Significant difference at $p < 0.02$ compared with control. (h) Quantitation of the myogenin expression level in gastrocnemius muscle of fasting mice. **Significant difference at $p < 0.02$ compared with control. Data are presented as means and SD based on three independent experiments ($n = 6$).

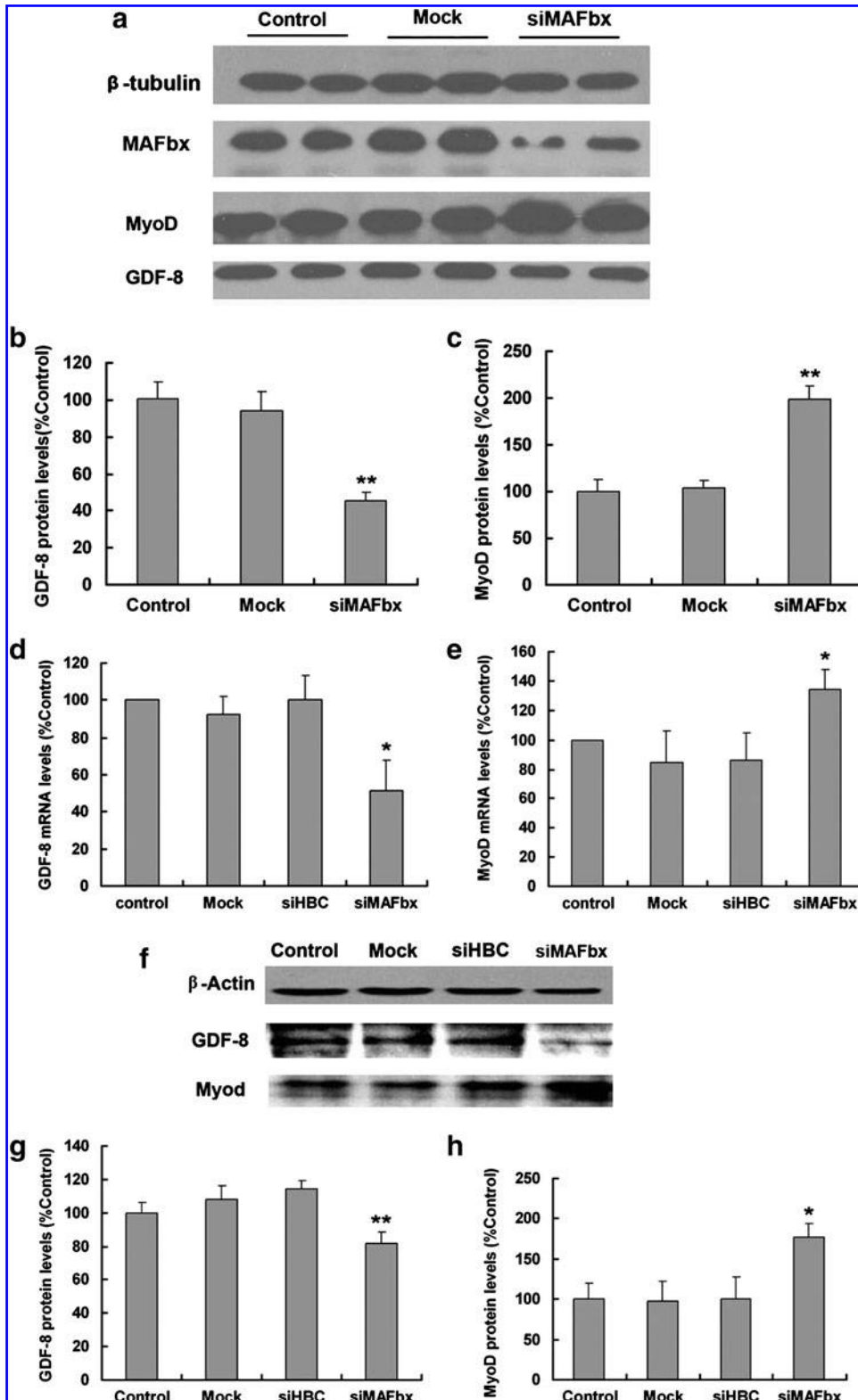


FIG. 7. Effects of adenovirus-delivered siRNA targeted against MAFbx on the expression of MyoD and GDF-8 in fasting mice and C2C12 cells. (a) Western blot analysis of MyoD and GDF-8 expression in gastrocnemius muscle of siMAFbx recombinant adenovirus-treated mice. Control, fasting mice injected with saline; Mock, fasting mice transduced with pDC312 recombinant adenovirus (empty vector) (all treatments, $n = 6$). (b) Quantitation of the GDF-8 expression level in gastrocnemius muscle of siMAFbx recombinant adenovirus-treated mice. **Significant difference at $p < 0.02$ compared with control. (c) Quantitation of the MyoD expression level in gastrocnemius muscle of siMAFbx recombinant adenovirus-treated mice. **Significant difference at $p < 0.02$ compared with control. (d) Quantitative RT-PCR analysis of the effect of siMAFbx on the mRNA level of GDF-8 in C2C12 cells. Control, uninfected C2C12 cells; Mock, cells infected with pDC312 recombinant adenovirus; siHBC, cells infected with siHBC recombinant adenovirus. *Significant difference at $p < 0.05$ compared with control. (e) Quantitative RT-PCR analysis of the effect of siMAFbx on the mRNA level of MyoD in C2C12 cells. * $p < 0.02$ compared with control. (f) Western blot analysis of MyoD and GDF-8 expression in C2C12 cells. (g) Quantitation of the GDF-8 expression level in C2C12 cells. **Significant difference at $p < 0.02$ compared with control. (h) Quantitation of the MyoD expression level in C2C12 cells. *Significant difference at $p < 0.05$ compared with control. Data are presented as means \pm SD based on three independent experiments.

siMAFbx recombinant adenovirus-treated mice. Western blot results (Fig. 7a) revealed that the GDF-8 expression level was decreased by 54.4% (Fig. 7b) whereas MyoD was increased by 52.2% compared with the saline and empty vector control groups (Fig. 7c). These findings demonstrated

that suppression of MAFbx expression by adenovirus-mediated RNA interference could improve muscle growth in fasting mice through an attenuation of the decrease in MyoD and downregulation of GDF-8 expression, in addition to directly blocking the degradation of muscle pro-

tein by decreasing the activity of ubiquitin–proteasome pathway.

We would expect to observe this effect in the C2C12 cell line as well. Indeed, results showed that in siMAFBx-infected C2C12 cells, GDF-8 expression at the mRNA level was decreased by 46.5% whereas the MyoD mRNA level was increased by 34.2% compared with the controls (Fig. 7d and e). These changes were further confirmed at the protein level using Western blots (Fig. 7f), where GDF-8 was decreased by 18.3%, whereas MyoD was increased by 42.4% relative to the controls (Fig. 7g and h). These results suggested that GDF-8 and MyoD could be two of the target genes regulated by MAFbx during differentiation of C2C12 cells.

Discussion

MAFBx has been recognized as a critical regulator of muscle atrophy (Palma *et al.*, 2008). Therefore, inhibition of MAFbx could be one of the approaches to clinically intervene in various conditions associated with muscle atrophy. This can be achieved by different means, such as by using antibody- and nucleic acid-based agents. RNA interference (RNAi) approaches based on synthetic siRNA or plasmid-mediated shRNAs have been widely used, but the high cost of synthesis, their low transfection efficiencies, and the adverse nature of the transient action have limited the application of these agents in clinical settings. Because adenovirus is relatively safe and is highly infectious, an adenovirus-based vector could be the better choice to deliver siRNA into mammalian cells (Shen *et al.*, 2003; Li *et al.*, 2007). In the present study, we developed an adenovirus-based strategy in which an adenovirus that expressed shRNA under the control of two promoters effectively suppressed MAFbx gene expression. We showed that adenovirally delivered MAFbx shRNA could lead to amelioration of muscle-wasting conditions and reduction in the loss of muscle mass in fasting mice. This action is gene specific, without the observed off-target effect.

It is becoming evident that proteolytic activities mediated by ubiquitin–proteasome, lysosomal, and calpain pathways as well as their interactions are involved in muscle proteolysis during atrophy. However, the accelerated rate of protein degradation in atrophying muscle occurs mainly through activation of the ubiquitin–proteasome pathway (Cao *et al.*, 2005). During this process, massive changes in the expression of some atrophy genes and growth factors have been shown to be involved, leading to muscle protein loss (Jackman and Kandarian, 2004). MAFbx is highly expressed during muscle atrophy and induces muscle protein degradation (Gomes *et al.*, 2001), but its direct targets remain to be determined. Consistent with the observation that a low level of MyoD expression is crucial for muscle loss (Rudnicki and Jaenisch, 1995), inhibition of MAFbx-mediated MyoD proteolysis prevents skeletal muscle atrophy *in vivo* (Lagirand *et al.*, 2009). Whether MAFbx could participate in the muscle-wasting conditions through other factors is not clear.

In our study, we provide further experimental evidence both *in vitro* and *in vivo* that downregulation of MAFbx expression could significantly increase the level of MyoD, suggesting that MyoD is one of the important targets for MAFbx-mediated protein degradation via the ubiquitin–

proteasome pathway. In addition, blockage of GDF-8 expression by an anti-GDF-8 antibody was shown to increase muscle mass in healthy adult mice (Jouliat *et al.*, 2003). GDF-8 could regulate myoblast differentiation by inhibiting MyoD activity and its gene expression via Smad3, resulting in the failure of myoblasts to differentiate into myotubes (Langley *et al.*, 2002). It has been shown that suppression of GDF-8 in cells and in normal and cachectic mice led to an increase in skeletal muscle mass of the mice (Liu *et al.*, 2008). There are also reports showing that GDF-8 could induce cachexia by activating the ubiquitin–proteasome pathway (McFarlane *et al.*, 2006). Our results show that the suppression of MAFbx expression by shRNA was accompanied by a decreased level of GDF-8 and an increased level of MyoD, which could suggest that MyoD is a negative regulator of GDF-8 in muscles.

Taken together, the present study provides information that not only better our understanding of the molecular mechanisms by which MAFbx functions in muscle cells but also suggests that targeting a muscle-specific E3 ubiquitin ligase at an early stage of muscle atrophy could be a preferred strategy for molecular and clinical intervention in the muscle-wasting pathological process.

Acknowledgments

The authors thank Dr. Paul Chu and Dr. Basam Z. Barkho for help during the preparation of the manuscript. The authors also thank Dr. David R. Engelke of the University of Michigan, for providing the plasmid pAVU6+27. This work was supported by a grant from the National High Technology Research and Development Program of China (863 Program) (no. 2007AA021505) and a grant from the National Natural Science Foundation of China (NSFC Grant no. 81021003).

Author Disclosure Statement

No competing financial interests exist.

References

- Attaix, D., Ventadour, S., Codran, A., Bechet, D., Taillandier, D., and Combaret, L. (2005). The ubiquitin–proteasome system and skeletal muscle wasting. *Essays Biochem.* 41, 173–186.
- Bodine, S.C., Latres, E., Baumhueter, S., Lai, V.K., Nunez, L., Clarke, B.A., Poueymirou, W.T., Panaro, F.J., Na, E., Dharmarajan, K., Pan, Z.Q., Valenzuela, D.M., DeChiara, T.M., Stitt, T.N., Yancopoulos, G.D., and Glass, D.J. (2001). Identification of ubiquitin ligases required for skeletal muscle atrophy. *Science* 294, 1704–1708.
- Bogdanovich, S., Krag, T.O., Barton, E.R., Morris, L.D., Whittemore, L.A., Ahima, R.S., and Khurana, T.S. (2002). Functional improvement of dystrophic muscle by myostatin blockade. *Nature* 420, 418–421.
- Cao, P.R., Kim, H.J., and Lecker, S.H. (2005). Ubiquitin–protein ligases in muscle wasting. *Int. J. Biochem. Cell Biol.* 37, 2088–2097.
- Dasarathy, S., Dodig, M., Muc, S.M., Kalhan, S.C., and McCullough, A.J. (2004). Skeletal muscle atrophy is associated with an increased expression of myostatin and impaired satellite cell function in the portacaval anastomosis rat. *Am. J. Physiol. Gastrointest. Liver Physiol.* 287, G1124–G1130.
- Gomes, M.D., Lecker, S.H., Jagoe, R.T., Navon, A., and Goldberg, A.L. (2001). Atrogin-1, a muscle-specific F-box protein

- highly expressed during muscle atrophy. *Proc. Natl. Acad. Sci. U.S.A.* 98, 14440–14445.
- Green, H.J., Reichmann, H., and Pette, D. (1982). A comparison of two ATPase based schemes for histochemical muscle fibre typing in various mammals. *Histochemistry* 76, 21–31.
- Jackman, R.W., and Kandarian, S.C. (2004). The molecular basis of skeletal muscle atrophy. *Am. J. Physiol. Cell Physiol.* 287, C834–C843.
- Joulia, D., Bernardi, H., Garandel, V., Rabenoelina, F., Vernus, B., and Cabello, G. (2003). Mechanisms involved in the inhibition of myoblast proliferation and differentiation by myostatin. *Exp. Cell Res.* 286, 263–275.
- Lagirand-Cantaloube, J., Cornille, K., Csibi, A., Batonnet-Pichon, S., Leibovitch, P.M., and Leibovitch, S.A. (2009). Inhibition of Atrogin-1/MAFbx mediated MyoD proteolysis prevents skeletal muscle atrophy *in vivo*. *PLoS One* 4, 1–11.
- Langley, B., Thomas, M., Bishop, A., Sharma, M., Gilmour, S., and Kambadur, R. (2002). Myostatin inhibits myoblast differentiation by down-regulating MyoD expression. *J. Biol. Chem.* 277, 49831–49840.
- Lecker, S.H., Jagoe, R.T., Gilbert, A., Gomes, M.O., Baracos, V., Bailey, J., Price, S.R., Mitch, W.E., and Goldberg, A.L. (2004). Multiple types of skeletal muscle atrophy involve a common program of changes in gene expression. *FASEB J.* 18, 39–51.
- Lee, S.J., and McPherron, A.C. (2001). Regulation of myostatin activity and muscle growth. *Proc. Natl. Acad. Sci. U.S.A.* 98, 9306–9311.
- Li, Y., Li, H., Yao, G., Li, W., Wang, F., Jiang, Z., and Li, M. (2007). Inhibition of telomerase RNA (hTR) in cervical cancer by adenovirus-delivered siRNA. *Cancer Gene Ther.* 14, 748–755.
- Liu, C.M., Yang, Z., Liu, C.W., Wang, R., Tien, P., Dale, R., and Sun, L.Q. (2008). Myostatin antisense RNA-mediated muscle growth in normal and cancer cachexia mice. *Gene Ther.* 15, 155–160.
- McFarlane, C., Plummer, E., Thomas, M., Hennebry, A., Ashby, M., Ling, N., Smith, H., Sharma, M., and Kambadur, R. (2006). Myostatin induces cachexia by activating the ubiquitin proteolytic system through an NF- κ B-independent, FoxO1-dependent mechanism. *J. Cell. Physiol.* 209, 501–514.
- McPherron, A.C., Lawler, A.M., and Lee, S.J. (1997). Regulation of skeletal muscle mass in mice by a new TGF- β superfamily member. *Nature* 387, 83–90.
- Palma, L., Marinelli, M., Pavan, M., and Orazi, A. (2008). Ubiquitin ligases MuRF1 and MAFbx in human skeletal muscle atrophy. *Joint Bone Spine* 75, 53–57.
- Rudnicki, M.A., and Jaenisch, R. (1995). The MyoD family of transcription factors and skeletal myogenesis. *Bioessays* 17, 203–209.
- Shen, C., Buck, A.K., Liu, X., Winkler, M., and Reske, S.N. (2003). Gene silencing by adenovirus-delivered siRNA. *FEBS Lett.* 539, 111–114.
- Stein, T.P., and Wade, C.E. (2003). Protein turnover in atrophying muscle: from nutritional intervention to microarray expression analysis. *Curr. Opin. Clin. Nutr. Metab. Care* 6, 95–102.
- Tintignac, L.A., Lagirand, J., Batonnet, S., Sirri, V., Leibovitch, M.P., and Leibovitch, S.A. (2005). Degradation of MyoD mediated by the SCF (MAFbx) ubiquitin ligase. *J. Biol. Chem.* 280, 2847–2856.
- Witt, S.H., Granzier, H., Witt, C.C., and Labeit, S. (2005). MURF-1 and MURF-2 target a specific subset of myofibrillar proteins redundantly: Towards understanding MURF-dependent muscle ubiquitination. *J. Mol. Biol.* 350, 713–722.

Address correspondence to:

Dr. Po Tien

Center for Molecular Virology

CAS Key Laboratory of Pathogenic Microbiology and Immunology

Institute of Microbiology

Chinese Academy of Sciences

Beijing 100101, People's Republic of China

E-mail: tienpo@sun.im.ac.cn

Received for publication March 24, 2010;

accepted after revision September 7, 2010.

Published online: December 2, 2010.